Wind Fragility of Roof Cladding and Trusses for Australian Contemporary Housing

Hao Qin
Graduate Student, Centre for Infrastructure Performance and Reliability, The University of Newcaslte, New South Wales, Australia

Mark G. Stewart
Professor, Centre for Infrastructure Performance and Reliability, The University of Newcaslte, New South Wales, Australia

ABSTRACT: This study develops a reliability-based fragility method to predict the roof damage for contemporary houses in non-cyclonic regions of Australia. The overloading of roof connections is considered as the limit state, and deemed to cause the roof sheeting loss and roof truss failures. A finite element method is employed to evaluate the wind uplift forces in roof connections. The finite element model consists of metal roof sheets and battens, timber roof trusses, wall top plates, and the cladding-to-batten, batten-to-rafter/truss and rafter/truss-to-wall connections. The finite element method is able to capture the load sharing and redistribution of the roof system. A Monte Carlo simulation in conjunction with the finite element method are employed to conduct the wind fragility assessment, which enables the probabilistic characterization of wind demands, uplift capacities and structural response for roof connections. The proposed fragility method is illustrated on a representative contemporary house built in suburbs of Brisbane and Melbourne. At a 500-year gust wind speed, considerable damage to roof cladding and trusses is predicted for the representative contemporary house in Brisbane with windward wall dominant openings.

1. INTRODUCTION

Roofing is generally the most vulnerable component of timber-frame houses under high wind loads, and its failure often initiates at and propagates through the roof connections (Henderson and Ginger 2007) that mainly include cladding-to-batten (CTB), batten-to-rafter/truss (BTR) and rafter/truss-to-wall (RTW) connectors. The damage of roof cladding and trusses due to wind uplift pressure may incur considerable economic losses for housing and impose safety threats on building occupants.

A wind fragility function typically expresses the damage state as a function of wind speed, which offers a convenient and effective metric to forecast the extent of wind damage, and therefore facilitates the risk assessment and mitigation for housing under extreme wind loading (Stewart et al. 2018). Contemporary houses in non-cyclonic regions of Australia typically have complex hip-roof geometries with metal roof sheeting installed. Screw fasteners and triple grip framing anchors are commonly used for the roof connections (Parackal et al. 2016; Satheeskumar 2016). The fragility analysis of roof cladding and trusses for Australian contemporary houses needs to account for the complex load sharing mechanism in evaluating the wind uplift forces, and the load redistribution after the initial failure of one or more roof connections.

In this study, a reliability-based fragility method was developed to assess the fragility of roof cladding and trusses for Australian contemporary houses under wind uplift pressures. A finite element (FE) model was employed to evaluate the wind uplift forces in the roof connections. The FE model consists of metal roof

sheets and battens, timber roof trusses, wall top plates, and the CTB, BTR and RTW connections. A Monte Carlo simulation (MCS) in conjunction with the FE method were employed to conduct the fragility assessment, which enables the probabilistic characterization of spatially varying wind uplift pressures, wind demands and uplift capacities for roof connections as well as the load redistribution and failure progression after local failures. The overloading of CTB, BTR and RTW connectors were considered as the limit states for the reliability-based fragility assessment. The fragility curves were developed to relate the extent of damage to roof cladding and trusses with gust wind speed. The developed fragility method was illustrated on a representative contemporary house built in suburbs of Brisbane and Melbourne.

2. RELIABILITY-BASED FRAGILITY METHOD

The fragility of a structural component or system is typically defined as the probability of damage state *DS* conditional on a given hazard *H*. The damage state herein is measured by the proportion of failed truss-to-wall connections, and the hazard is corresponding to the gust wind speed. The wind fragility is therefore the extent of damage to truss-to-wall connections, R_{loss}, at a given gust wind speed v, expressed as

$$\Pr(DS|H) = \Pr[DS = R_{loss}|H = v] \qquad (1)$$

The failure of a single roof connection is governed by the following limit state function

$$g = R - (W - D_L) \qquad (2)$$

where R represents the resistance of the considered connection, and W is the wind uplift force in the roof connection. The dead load arising from the weight of roof components is D_L. A connection is overloaded (i.e. failure) if $g \leq 0$. In this study, the uplift loads acting on the roof connections are obtained by using a FE approach, which takes into account the load sharing and redistribution under the spatially varying wind uplift pressure. The details of the FE modelling are described in Section 5. The dead load is considered in the FE modelling by specifying the density of roof components. The failure of a single roof sheet occurs when the number of failed fasteners on the roof sheet N_f exceeds a threshold value N_{cr}. A BTR connection failure is modelled as if all roof fasteners connected to the batten have failed. The sheet failure threshold value (N_{cr}) is equivalent to the sheet failure criterion (SFC) defined in Stewart et al. (2018), which is probabilistically modelled as a triangular distribution. A roof truss failure is deemed to occur if any of its RTW connection overloaded.

A MCS in conjunction with the FE approach are employed in this study to evaluate the wind fragility for roof cladding and trusses, which enables the stochastic characterization of spatially varying wind uplift pressures, uplift forces in roof connections, failure progression and load redistribution, and evolution of internal pressure with increasing sheeting loss. In each run of the MCS, the spatially distributed wind pressures and structural resistances of roof connections are randomly generated as the input to the FE model of the roof system. The wind uplift forces in the roof connections are then obtained from the FE analysis, and the failure of a single connection is checked by the limit state function given by Eq. (2). Any overloaded (failed) roof connections are then deactivated in the FE model, and the FE analysis is further conducted to evaluate the load redistribution and failure progression of other connections. The MCS and FE approach proposed in the present study enables the development of two fragility curves: (i) the extent of roof sheeting loss, and (ii) proportion of roof truss failures.

3. REPRESENTATIVE CONTEMPORARY HOUSE

A representative contemporary house built in the Australian suburbs of Melbourne and Brisbane is used to illustrate the fragility method proposed in the present study. The dimension, shape and construction type of the house were determined by field surveys completed by the Cyclone Testing Station (CTS) at James Cook University (JCU) (Parackal et al. 2016). The median values of house plans and features from the survey such as

footprint dimensions, roof pitch and wall heights were selected to determine the configuration of the representative contemporary house. Figure 1 shows the 3D and plan view of the representative one-story house. It is a timber-framed construction with 21.5° timber roof trusses at 600 mm spacings on a complex hip-end roof. Trusses are arranged with standard trusses in the middle part of the roof and jack trusses connected to truncated girder trusses at the hip ends. Roof cladding is 762 mm wide corrugated metal sheeting. Metal top-hat battens are attached to timber roof trusses at 900 mm spacings.

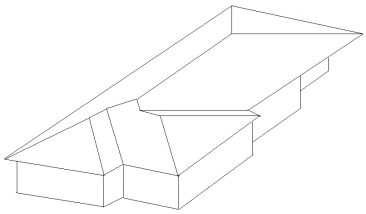

(a) 3D view

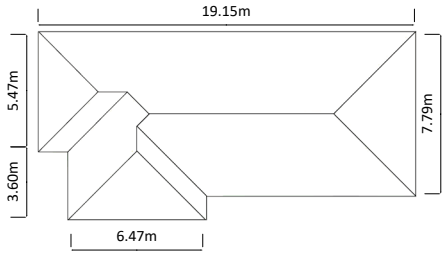

(b) Plan view

Figure 1: Representative contemporary house.

4. WIND LOADING AND CONNECTION RESISTANCE

4.1. Wind uplift load

The wind uplift load (W) is modelled probabilistically as (e.g. Stewart et al. 2018)

$$W = \lambda \cdot M \cdot A \cdot (C \cdot T \cdot E^2 \cdot D^2 \cdot G \cdot \frac{\rho}{2}) \cdot v^2 \quad (3)$$

where v is the maximum 0.2 second gust velocity at 10m height in Terrain Category 2 (i.e. open terrain defined in Australian wind loading standard AS/NZS 1170.2 2011); λ is a factor accounting for wind loading modelling inaccuracies and uncertainties; M accounts for wind tunnel modelling inaccuracies such as incorrect Reynolds number, building details, and site modelling; A is the loaded area uncertainty arising from geometric uncertainties of the cladding fastener, batten and truss spacing; C is the quasi-steady pressure coefficient, which is a combination of external (C_{Pe}) and internal pressure coefficient (C_{Pi}); T is the shielding factor; E is a terrain height multiplier that accounts for the exposure and height of the building considered; D is a factor accounting for wind directionality effects; G is a factor that accounts for gusting effects, and ρ is the density of air. These parameters, except for C, are assumed to follow a lognormal distribution (Henderson and Ginger 2007) with estimated means and coefficient of variations (COV) listed in Table 1 that are derived from the statistics given in Holmes (1985) and Stewart et al. (2018). The nominal values can be obtained from AS/NZS 1170.2 (2011).

Table 1. Statistical parameters for wind uplift load.

Parameter	*Mean*	*COV*
λ/λ_N	*1.0*	*0.10*
M/M_N	*1.0*	*0.10*
A/A_N	*1.0*	*0.05*
E/E_N	*0.95*	*0.10*
T/T_N	*1.0*	*0.10*
D/D_N	*1.0*	*0.00*
G/G_N	*1.0*	*0.05*
ρ/ρ_N	*1.0*	*0.02*

Wind tunnel testing was employed in this study to evaluate the external pressure coefficients in Eq. (3). The spatially and temporarily varying external pressure coefficients for the roof surface were measured in a wind tunnel test conducted in the Boundary Layer Wind Tunnel at JCU. The peak external pressure coefficients at a total of 320 pressure tap locations for each wind direction were modelled by a Gumbel probability distribution with the scale and location parameters estimated using a maximum likelihood method based on the wind tunnel

observations. More details about the wind tunnel test can be found in Parackal et al. (2016).

The failure of windows, doors and roof sheets during an extreme wind event may change the internal pressure and therefore affect the roof damage assessment. In this paper, two typical scenarios are assumed for the internal pressure evaluation, namely, dominant openings existing on the windward wall and effectively sealed building without any wall openings. Both of the two scenarios consider the increasing roof openings due to damage progression of roof sheeting. The internal pressure coefficient is assumed to follow a normal distribution with a COV of 0.33 (e.g. Lee and Rosowsky 2005). For the later scenario, the mean internal pressure coefficients would equal to the average of external pressure coefficients at roof openings. Derived from the mass conservation theory (Holmes 2015), the mean internal pressure coefficient for the former scenario is calculated as

$$C_{Pi} = \frac{C_{PW}}{1+(\frac{A_R}{A_W})^2} + \frac{C_{PR}}{1+(\frac{A_W}{A_R})^2} \quad (4)$$

where C_{PW} is the average of external pressure coefficients at windward wall openings and C_{PR} is the average of external pressure coefficients at roof openings; A_W is the total size of wall openings and A_R is the total size of roof openings.

4.2. Connection resistance

The representative contemporary house is installed with corrugated metal sheeting secured by screw fasteners at every 2nd corrugation of the roof edge and every 3rd or 4th corrugation for other regions of the roof. Metal top-hat 40 battens are used as roof battens and secured to every truss at 900 mm spacings (Parackal et al. 2016). The resistances for CTB and BTR connectors are modelled as random variables and the failure modes considered are (i) pull-over and (ii) pull-out failures. Both the pull-over and pull-out capacities of CTB and BTR connectors are assumed to follow a lognormal distribution (Henderson and Ginger 2007). The statistical parameters for the resistances of CTB and BTR connectors are listed in Table 2, which were derived from laboratory tests and summarized in Stewart et al. (2018). The connection resistances are assumed to be statistically independent and taken as the lower of randomly generated pull-out and pull-over strengths.

Triple grip connections (see Fig. 2) are typically used for the RTW connectors for Australian contemporary houses. The timber species for the truss is typically Australian radiata pine, and two types of fasteners, i.e. hand nails and gun nails, are used for the triple grip connections. The triple grip connection behaviour under uplift loads is captured by a piecewise-linear force-displacement relationship with its model parameters probabilistically characterized based on test data in Satheeskumar (2016). Figure 3 depicts the piecewise-linear model for the behaviour of triple grip RTW connectors in the vertical direction (i.e. y shown in Fig. 2). In Fig. 3, F_y is the yield load; k_0 is the initial secant stiffness; δ_y is the displacement at yielding; F_u is the peak load (considered as the uplift capacity for the connection); δ_u is the displacement at peak load, and δ_{max} is the displacement of triple grip connection at complete separation from the rafter.

Table 2. Statistical parameters for resistances of CTB and BTR connectors.

	Failure mode	*Mean*	*COV*	*Distribution type*
CTB	*Pull over*	*1.2kN*	*0.30*	*Lognormal*
	Pull out	*1.2kN*	*0.20*	
BTR	*Pull over*	*4.5kN*	*0.15*	*Lognormal*
	Pull out	*5.5kN*	*0.20*	

The overloading of roof connections ($F \geq F_u$) is considered as the limit state for the current reliability-based fragility method. Thus, the connection behaviour after peak load is neglected in the FE analysis and it is assumed that the overloaded RTW connector tends to lose its load carrying capacity very quickly. A much higher compression stiffness (i.e. 20 kN/mm) is assumed for the RTW connector in the vertical (y) direction. Three major parameters, i.e. k_0, F_u and δ_u, are used to define the piecewise-linear model in Fig. 3. All these parameters are assumed to follow lognormal

distributions with the mean and COV values obtained from the test data (Satheeskumar 2016). The statistical parameters of k_0, F_u and δ_u for triple grip connections fastened using hand nails and gun nails are listed in Table 3. The yield force (F_y) is defined as two-thirds of F_u based on the averaged ratio of F_y to F_u in the test data. The correlation coefficients between these three model parameters are also obtained from the test data as shown in Table 4, and when conducting the fragility analysis, the lognormally correlated parameters are sampled in the MCS using Nataf transformation (Liu and Der Kiureghian 1986) for the calculation of the covariance matrix.

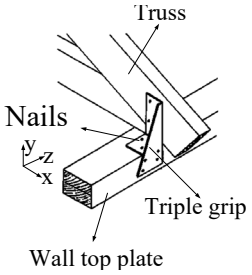

Figure 2: Triple grip RTW connector.

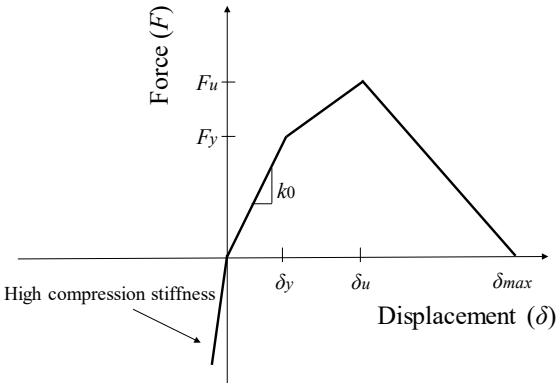

Figure 3: Piecewise-linear force-displacement relationship for triple grip RTW connectors

Table 3. Statistical parameters of the piecewise-linear model for RTW connectors.

(a) Hand nail triple grip

RTW parameters	*Mean*	*COV*	*Distribution type*
k_0 (kN/mm)	*0.44*	*0.17*	*Lognormal*
F_u (kN)	*4.85*	*0.11*	
δ_u (mm)	*19.49*	*0.12*	

(b) Gun nail triple grip

RTW parameters	*Mean*	*COV*	*Distribution type*
k_0 (kN/mm)	*0.34*	*0.15*	*Lognormal*
F_u (kN)	*3.80*	*0.11*	
δ_u (mm)	*19.95*	*0.18*	

Table 4. Correlation coefficients between piecewise-linear model parameters for RTW connectors.

Parameters	*Correlation coefficient*	
	Hand nail triple grip	*Gun nail triple grip*
k_0 and F_u	*0.63*	*0.45*
k_0 and δ_u	*−0.27*	*−0.16*
F_u and δ_u	*0.12*	*0.14*

5. FE MODELLING OF ROOF SYSTEM

A FE approach using commercial FE software ANSYS (ANSYS Inc. 2013) is proposed to evaluate the wind uplift loads acting on roof connections and load redistribution after the failure of one or more connections. The FE approach in conjunction with MCS enables an simulation for wind fragility assessment considering the progressive failure of roof connections. As shown in Fig. 1, the representative contemporary house has a complex hip-roof geometry that requires excessive cost in both FE modelling and computation (e.g. CPU hours) for the reliability-based fragility assessment. To reduce the cost in FE modelling and computation, the proposed FE approach in this study models the roof cladding and trusses separately, and only critical roof trusses are modelled.

The roof cladding FE model consists of corrugated metal roof sheets, metal top-hat battens, CTB and BTR connectors, which is employed in the MCS analysis to evaluate roof sheeting loss under the spatially varying wind uplift pressure. The roof truss FE model mainly comprises a critical proportion of the timber trusses in the representative contemporary house, which includes 14 standard trusses, 2 truncated standard trusses and 1 truncated girder truss as shown in Fig. 4. These modelled trusses cover most of the critical trusses (i.e. trusses that are

more likely to fail under wind uplift) in the roof system. Two additional truncated girder trusses depicted in solid line as shown in Fig. 4, though not included in the FE modelling, are also considered in the fragility assessment using a simple tributary area approach as they are among the most vulnerable trusses in the roof system. In a single MCS run, the wind uplift loads acting on the BTR connectors obtained from the roof cladding FE model are subsequently applied to the roof truss FE model for truss failure assessment.

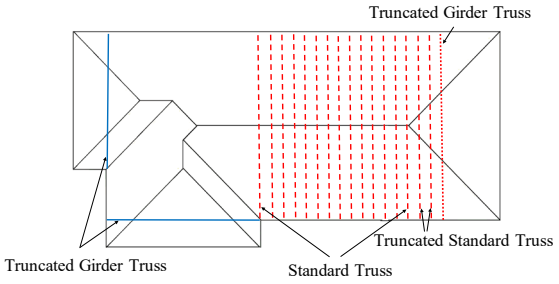

Figure 4: The critical trusses modelled in the FE analysis.

5.1. Roof cladding FE modelling

The FE model of the roof cladding layout containing 75 corrugated metal roof sheets is shown in Fig. 5(a). Four-node quadrilateral shell elements including both bending and membrane stiffness are used to model the corrugated metal sheet with six degrees of freedom at each node. The FE model of a typical corrugated metal roof sheet installed on the representative house is depicted in Fig. 5(b). The corrugated metal sheet has a width of 762 mm, base metal thickness (BMT) of 0.42 mm and crest height of 22 mm. Roof sheets with other shapes are configured by trimming the typical sheets at ridgelines and hips as shown in Fig. 5(a).

The material properties for the corrugated metal sheets are assumed to be isotropic and linear-elastic with a Young's modulus of 220,000 MPa and a Poisson's ratio of 0.3 (Lovisa et al. 2013). Two-node beam elements are used to model the metal top-hat roof battens with material and section properties obtained from manufacture's specifications (Lysaght 2014). It is assumed that the CTB and BTR connectors no longer carry any loads when corresponding uplift forces exceed their pull-out and/or pull-over resistances, and the overloaded connections are then deactivated in the roof cladding FE model for further analysis of load redistribution and failure progression. The CTB and BTR connectors are approximately modelled by linear spring elements. The stiffness of the linear spring elements is also assumed to follow a lognormal distribution with a mean value of 300 N/mm and 1800 N/mm (Satheeskumar 2016) for CTB and BTR connectors, respectively. A COV value of 0.20 is assumed for the stiffness variability due to a lack of relevant data. The roof trusses are not modelled in the roof cladding FE model and flexible supports are assumed to represent the attachment points of batten fasteners to rafters.

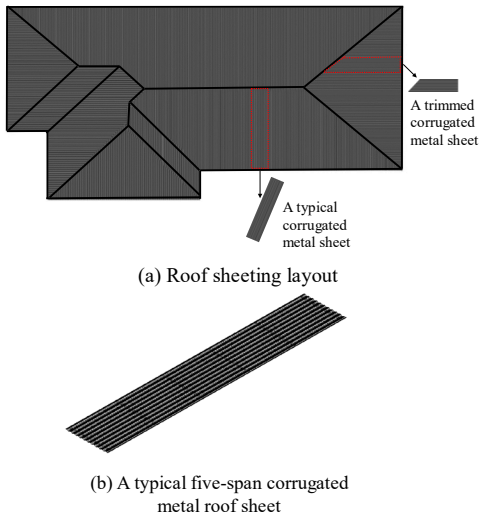

Figure 5: Roof cladding FE model.

5.2. Roof truss FE modelling

A total of 17 timber roof trusses are modelled in the roof truss FE model, which contains most of the critical trusses in the roof system. Two-node beam elements with a rectangular section of 90 mm × 35 mm are used to assemble the timber trusses, and the material properties of the truss members are assumed to be isotropic and linear-elastic with a Young's modulus of 10,000 MPa and a Poisson's ratio of 0.37 (Satheeskumar 2016). The same beam elements are used to model the double ribbon wall top plates at each side of the trusses but with a section of 70 mm × 90 mm

(twice of each top plate). The wall frame below the top plates are not modelled and flexible supports are assumed to represent the attachment points of top plates to wall studs.

The triple grip connections as shown in Fig. 2 are used for the RTW connectors, which are modelled by three non-linear spring elements to characterize the connection behaviour in uplift and shear. The force-displacement relationship for the spring element in the vertical direction (y direction in Fig. 2) is probabilistically characterized by the piecewise-linear model as described in Section 4.2. The load-deflection behaviour for the spring elements in x (i.e. along the truss) and z (i.e. normal to the truss plane) directions as shown in Fig. 2 are assumed to be deterministic and the mean force-displacement curves obtained from test data are used for these two spring elements (Satheeskumar 2016). The metal battens are also assembled in the roof truss FE model as shown in Fig. 6.

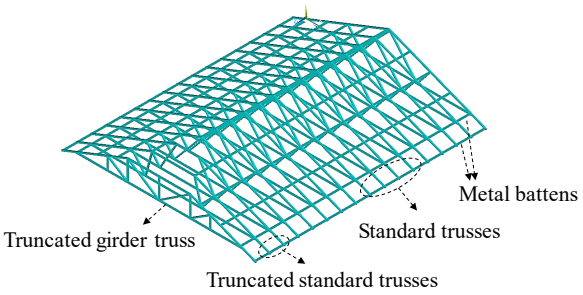

Figure 6: Roof truss FE model.

In one MCS run, the uplift forces in BTR connectors obtained from the roof cladding FE model are applied to the roof truss FE model to evaluate the failure of RTW connectors, which accounts for the effect of failure progression of CTB and BTR connectors on the vertical load transfer to RTW connectors. Besides the uplift loads from BTR connectors, additional point loads obtained from the roof cladding FE model in the same MCS run are applied to the bottom chord of the truncated girder truss. These additional loads are derived from the sampled wind uplift loads acting on the hip and jack trusses supported by the truncated girder truss.

6. FRAGILITY RESULTS

The fragilities up to gust wind speed of 80m/s are calculated for roof cladding and trusses considering two wall opening scenarios: (i) presence of windward wall dominant openings and (ii) effectively sealed building without any wall openings. A total of 1800 MCS runs are conducted for the fragility assessment considering the random building orientation. The MCS and the FE approach for the representative contemporary house includes 1646 CTB, 532 BTR and 38 RTW connectors. The design considerations for RTW connectors for Brisbane and Melbourne houses based on AS4055 (2012) and AS 1684.2 (2010) are shown in Table 5. Note that CTB and BTR connections are identical for Brisbane and Melbourne houses.

Table 5. Design and construction considerations for RTW connectors (AS4055 2012, AS 1684.2 2010).

Wind classification	*Location*	*RTW connectors*	
		Standard truss	*Truncated girder truss*
N1	*Melbourne*	*One gun nail triple grip*	*One gun nail triple grip*
N2	*Melbourne/ Brisbane*	*One gun nail triple grip*	*Two gun nail triple grips*
N3	*Brisbane*	*One hand nail triple grip*	*Two hand nail triple grips*

The fragility curves for the representative contemporary house built in the suburbs of Brisbane and Melbourne considering two wall opening scenarios are shown in Fig. 7. The design wind speed corresponding to a 500-year return period for Brisbane is 57 m/s (AS/NZS 1170.2 2011). At this gust wind speed, the mean roof sheeting loss for the representative contemporary house is 4.5% with windward wall dominant openings and only 0.1% for the scenario without any wall openings. While the latter loss is insignificant, the former may result in a considerable economic loss. The mean proportion of roof sheeting loss at the 500-year gust wind speed of Melbourne, i.e. 45 m/s (AS/NZS 1170.2

2011), is negligible for both wall opening scenarios.

The mean proportion of roof truss failures for the representative contemporary house built in Brisbane at the 500-year design wind speed (i.e. 57 m/s) with windward wall dominant openings is 3.3% and 0.6% for design wind classifications N2 and N3, respectively. At the 500-year gust wind speed for Melbourne (i.e. 45 m/s), the mean proportion of roof truss failures for suburban house in Melbourne with windward wall dominant openings is 0.2% and 0.1% for wind classifications N1 and N2, respectively, which is deemed as negligible damage.

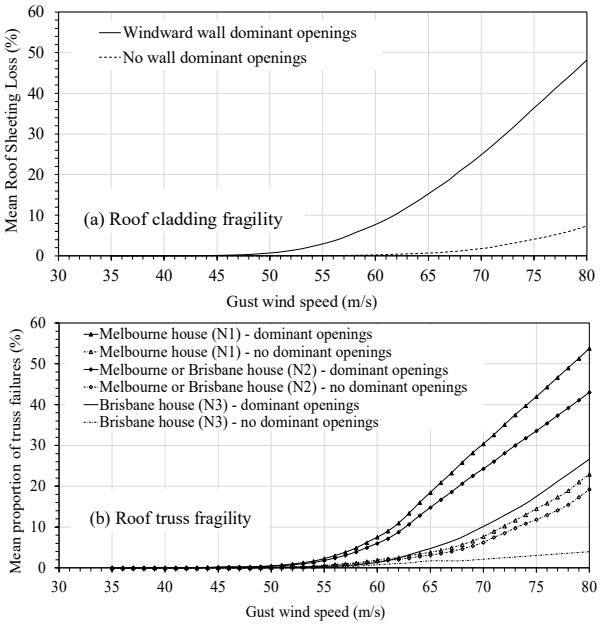

Figure 7: Fragility curves for roof cladding and trusses for two wall opening scenarios.

7. CONCLUSIONS

This paper developed a reliability-based fragility method to evaluate the roof sheeting loss and roof truss failure for contemporary houses subjected to extreme winds in non-cyclonic regions of Australia. The fragility analysis results reveal that, if no wall dominant opening exists, the mean proportions of roof sheeting loss and roof truss failures are negligible under a 500-year return period wind speed. When subjected to windward wall dominant openings, considerable roof sheeting loss and roof truss failures are predicted at the 500-year gust wind speed for the Brisbane house.

8. REFERENCES

ANSYS Inc (2013). *ANSYS Mechanical APDL Introductory Tutorials*. Canonsburg, PA; USA.

AS 1684.2 (2010). *Residential timber-framed construction*. Standards Australia, Sydney.

AS 4055 (2012). *Wind Loads for Housing*. Standards Australia, Sydney.

AS/NZS 1170.2 (2011). *Structural Design Actions, Part 2: Wind Actions*. Standards Australia, Sydney.

Henderson, D. J. and Ginger, J. D. (2007). "Vulnerability model of an Australian high-set house subjected to cyclonic wind loading". *Wind and Structures*, 10(3), 269-285.

Holmes, J.D., (2015). *Wind loading of structures*. 3rd Edition, CRC Press Boca Raton, Florida, USA

Lee, K. H. and Rosowsky, D. V. (2005). "Fragility assessment for roof sheathing failure in high wind regions". *Engineering Structures*, 27(6), 857-868.

Liu, P. L. and Der Kiureghian, A. (1986). "Multivariate distribution models with prescribed marginals and covariances". *Probabilistic Engineering Mechanics*, 1(2), 105-112.

Lovisa, A. C., Wang, V. Z., Henderson, D. J. and Ginger, J. D. (2013). "Development and validation of a numerical model for steel roof cladding subject to static uplift loads". *Wind and Structures*, 17(5), 495-513.

Lysaght (2014). *TOPSPAN Design and Installation Guide for Building Professionals*. Bluescope Lysaght, Australia.

Parackal, K. I., Humphreys, M. T., Ginger, J. D. and Henderson, D. J. (2016). "Wind Loads on Contemporary Australian Housing". *Australian Journal of Structural Engineering*, 17(2), 136-150.

Satheeskumar, Navaratnam (2016). *Wind load sharing and vertical load transfer from roof to wall in a timber-framed house*. PhD thesis, James Cook University, Australia.

Stewart, M. G., Ginger, J. D., Henderson, D. J. and Ryan, P. C. (2018). "Fragility and climate impact assessment of contemporary housing roof sheeting failure due to extreme wind". *Engineering Structures*, 171, 464-475.